Microstructure formation in a thick polymer by electrostatic-induced lithography

2013 J. Micromech. Microeng. 23 035018

(http://iopscience.iop.org/0960-1317/23/3/035018)

J. Micromech. Microeng. **23** (2013) 035018 (8pp) doi:10.1088/0960-1317/23/3/035018

Microstructure formation in a thick polymer by electrostatic-induced lithography

G Liu[1,2], W Yu[1], H Li[1,2], J Gao[1], D Flynn[3], R W Kay[3], S Cargill[3], C Tonry[4], M K Patel[4], C Bailey[4] and M P Y Desmulliez[3]

[1] State Key Laboratory of Applied Optics, Changchun Institute of Optics, Fine Mechanics & Physics, Chinese Academy of Sciences, No. 3888, Dongnanhu Road, Changchun, Jilin, People's Republic of China
[2] Graduate School of the Chinese Academy of Science, Beijing, 10039, People's Republic of China
[3] MIcroSystems Engineering Centre (MISEC), School of Engineering & Physical Sciences, Heriot-Watt University, Edinburgh EH14 4AS, UK
[4] School of Computing and Mathematical Sciences, University of Greenwich, Old Royal Naval College, Park Row, London SE10 9LS, UK

E-mail: yuwx@ciomp.ac.cn and m.desmulliez@hw.ac.uk

Received 6 October 2012, in final form 4 January 2013
Published 1 February 2013
Online at stacks.iop.org/JMM/23/035018

Abstract
This article demonstrates the manufacturing of microstructures in a thick polymer using electrostatic-induced lithography. Unlike previous work reported elsewhere, it focuses on the fabrication of structures from meso- to micro-scale. The electrostatic-induced lithography technique is proven to work with not only dc voltage but also ac voltage. Microstructures including microchannels, sinusoidal surface profile microstructures, waveguide core, microlens array and binary Fresnel zone plate have been successfully fabricated. The aspect ratio obtained for some samples is up to 4.5:1. The whole fabrication process is fast, cost-effective in terms of the simple experimental setup and no photosensitive material is needed. This process is expected to find applications in microfluidics, photonics or micro-opto-electro-mechanical systems.

(Some figures may appear in colour only in the online journal)

1. Introduction

In recent decades, a large body of literature has been reported on the formation of self-assembled and ordered structures in polymers induced by electrostatic forces [1–16]. The physical explanation and simulation of the formation of specific structures induced by electrostatic pressure have also been reported [17–28]. In all these articles, a polymeric film with a thickness of around 100 nm was used to grow structures with dimensions ranging from sub-micron to several microns. However, this paper concentrates on the feasibility of this technology, called electrostatic-induced lithography, for the fabrication of deep microchannels and wafer bumps, to name but a few applications, at the meso-scale and micrometer scale.

Electrostatic-induced lithography offers several advantages over traditional photolithography techniques. Firstly, there is no expensive optical equipment involved since no UV light source unit and corrective optics are needed. Secondly, any polymer whose viscosity decreases at elevated temperature, in principle, should be suitable for this technique. The fabrication cost would thereby be greatly reduced in the case of manufacturing of tall structures because thick photosensitive photo-resists are quite expensive. Thirdly, there is no development process needed due to the one-step pattern formation after annealing of the polymer. Comparing with other prevalent methods such as soft lithography and injection molding, electrostatic-induced lithography has also a number of advantages. Firstly, the shape as well as the aspect ratio of the fabricated microstructures are absolutely

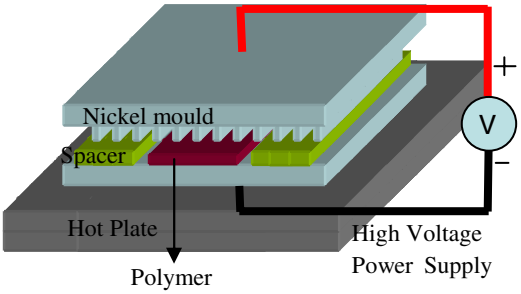

Figure 1. Experimental setup for the fabrication of microchannels in the polymer by electrostatic-induced lithography method.

determined and limited by the mold for soft lithography and injection molding. However for electrostatic-induced method, the shape of the fabricated microstructure can be flexibly controlled by carefully adjusting the process parameters (the polymer thickness, the air gap between the mold and the polymer and so on) to form the binary as well as continuous surface profile. Besides, the aspect ratio of the fabricated microstructures also can be flexibly tuned. The other advantage of electrostatic lithography is that the surface of the fabricated microstructures is much smoother than that obtained by soft lithography and injection molding due to the formation of microstructures by the flow of the fluid for the case when the process is conducted in a non-contact mode. For soft lithography and injection molding, the surface roughness of the manufactured structure is limited by that of the mold. The smooth surface is important for photonics, optics, tissue engineering, genetics, biomedicine and microfluidics. In particular for microfluidics, the smooth surface is helpful to avoid unnecessary energy losses as the fluid flows through microchannels. It is all these advantages of electrostatic-induced lithography over other prevalent methods that makes it a very attractive method and have a great potential to be applied for microelectromechanical systems (MEMS) and microfluidics applications.

This paper reports the preliminary work carried out to demonstrate the processing capability of this technology. A brief review of the previous work in electrostatic-induced lithography as well as the motivation behind the current work is presented followed by the fabrication method and the materials used. The fabrication results of some samples and their characterization are then presented. Finally, conclusions and future work as well as possible applications are suggested.

2. Materials and method

The experimental setup used in this work is illustrated in the schematic given in figure 1. A nickel-based microchannel plate fabricated by the UV-LIGA process and shown in figure 2 is to be used as a master [29]. The microchannel considered has a width of 100 μm for a depth of 76 μm and the verticality of the walls is around 88°. In this process, a hot plate is used to heat the polymer to a temperature beyond the glass transition temperature. A glass plate is used as a spacer to control the gap between the two electrodes although a high

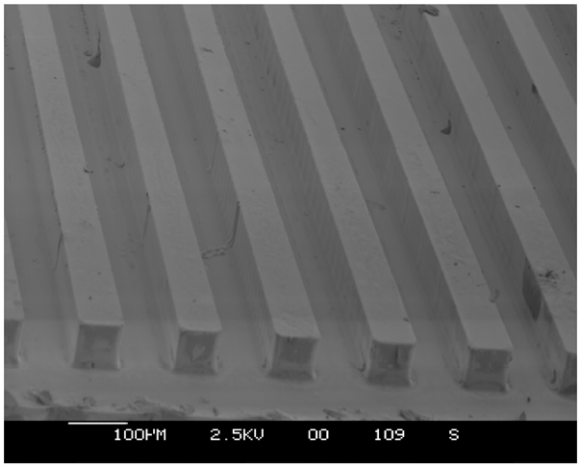

Figure 2. The nickel mould fabricated by the UV-LIGA process used in this experiment.

precision machine could be used to control the gap between the master and the replicated structure in real time. A novolac-based polymer of glass transition temperature of around 100° C (AZ9260 photoresist from Clariant (Clariant Co., Charlotte, NC) and a thickness of around 25 μm was coated onto a pre-cleaned 3 inch glass wafer by spin coating. A multi-layered Ti/Cu/Ti metal thin film, with a thickness of 300 nm, was deposited by an e-beam evaporator to render the glass wafer electrically conductive. An electrical potential difference was then applied between the nickel master electrode and the glass wafer as depicted in figure 1. The formation of the structure occurs during the annealing of the polymeric film when the temperature exceeds the glass transition temperature of the polymer.

3. Fabrication results and discussions

The experiment was conducted with the following parameters. A dc voltage of 1 000 V was applied and a hotplate was used to heat the polymers at a temperature of 120 °C. A glass plate with a thickness of around 85 μm is used to control the gap between the top electrode and the polymer. Figure 3 shows the fabricated microchannels in the polymer for an annealing time of 1 h. The results clearly depict the accuracy of the approach in terms of uniformity as well as the accuracy of the method. Here, the microchannel's width of 100 μm matches the one of the master. Furthermore, the developed height of these channels was around 83 μm for an initial polymer thickness of around 25 μm, thereby allowing the possibility to produce structures of height higher than those usually permissible by the manufacturers' recommendations. From the figures, there is still some polymer of thickness of around 10 μm remaining in the central area of the channels. One possible reason for this is that the annealing time was not long enough implying that some of the polymer did not have sufficient time to migrate fully. However, the more plausible reason for this behavior is that the gap was not large enough to accommodate the whole volume of the polymer to fully form the channels before reaching the surface of the master. Indeed the polymer can be seen to have touched the top electrode as

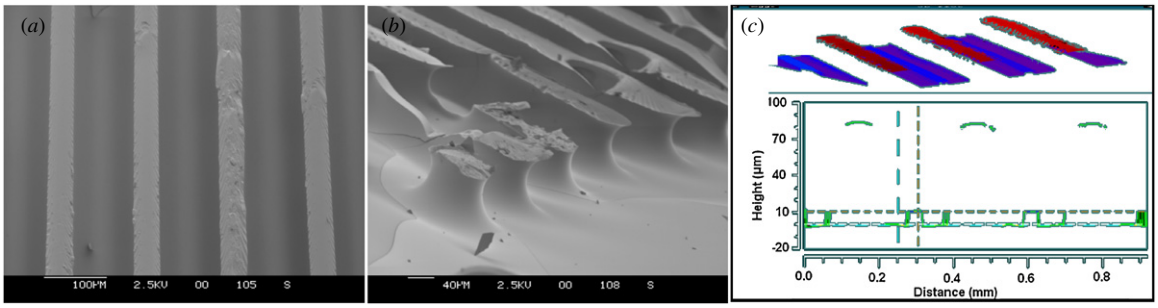

Figure 3. Scanning electron microscope (SEM) images and surface profile of the fabricated microchannels with a width of 100 μm measured using the Zygo optical interferometer NewView^{TM} 700 s. (*a*) Top view of the fabricated microchannels imaged by SEM, (*b*) side view of the exit end of the fabricated microchannels imaged by SEM, (*c*) 3D (top) and 2D (bottom) surface profile of the fabricated microchannels measured by the optical interferometer indicated a verticality of the walls of around 70°.

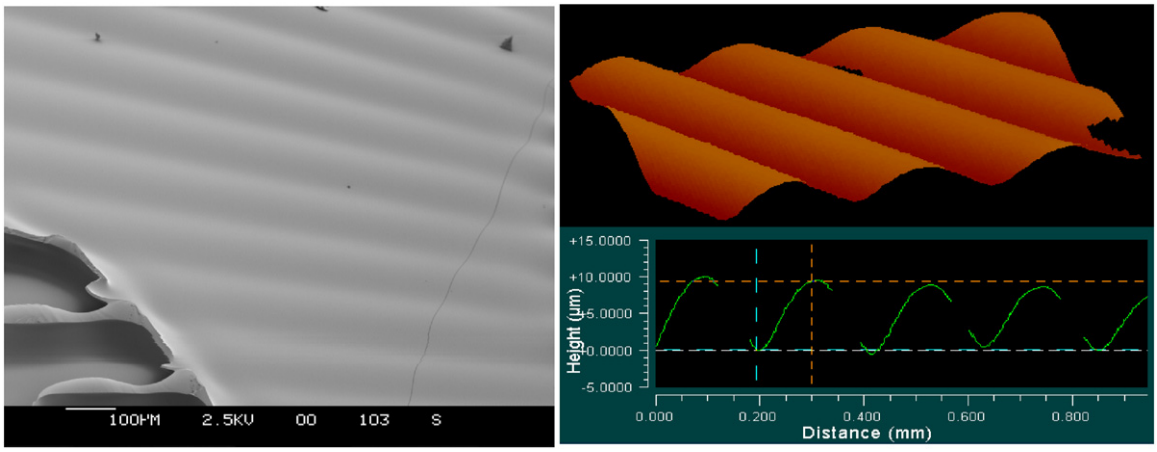

Figure 4. SEM image of the microchannels at their end (left) and the continuous surface relief structure measured by the Zygo optical interferometer (right).

shown in figure 3(*a*), where the top surface of the structures is quite flat. Had the initial thickness of the polymer been less, it is quite possible that the same channel height could have been attained without any polymer being left within the channel. Figure 3(*b*) depicts the scanning electron microscope (SEM) image of the edges of the microchannels at the edge of the master. As can be seen, the microchannels have a relatively straight wall (further confirmed by the optical profilometric measurement in figure 3(*c*)) and the surface of these sidewalls is also quite smooth. This is important for the microfluidic channel to ensure unnecessary pressure losses or a reduction in flow velocities. The wall at the end of the structures has a relatively large slope as too much of the polymer has migrated to this area from outside the microchannel. To avoid this, it is possible to control the straightness of the formed structure by carefully defining the spacing. In addition, the breakage of the structure, shown in figure 3(*b*), occurred during the separation process of the master from the wafer and suggests that the surface of the master should be modified to have a low surface energy to avoid any strong adhesion with the polymer during the replication process.

Furthermore, microstructures with continuous surface profile can also be fabricated by this method using the same nickel master. Figure 4 (right) shows the SEM image and the 3D surface profile measured by the Zygo optical interferometer NewView^{TM} 700 s. The formed microstructures have a height of around 9 μm. The ability to fabricate microstructures with a continuous surface relief structure makes the electrostatic-induced lithography a possible method to fabricate some contoured optical structures in polymer like sinusoidal gratings, e.g. Fresnel zone plates. Therefore, with a properly designed master, it is possible to create, in a single-step process, continuous profile structures such as those presented in figure 4 and 2.5D structures such as the microchannels shown in figure 3.

Besides microchannels, other microstructures in different materials have also been demonstrated by electrostatic-induced lithography. Figure 5 shows the core of an optical waveguide of diameter of 50 μm and height of 10 μm fabricated in the UV-cured polymer LightLink^{TM} XP-6701 (A–Z) Core (Rohm and Haas Electronic Materials LLC). The detailed fabrication process parameters can be found in [30]. The fabricated waveguides have a round shape and the surface is pretty smooth which is helpful to reduce optical losses. However, the end of the waveguide is not straight and has a large slope, which could be cut away by laser or dicing machine to make it straight so that the light can be guided in easily. Figure 6 shows a square pillar array with a diameter of 100 μm and a height of 20 μm fabricated in novolac-based polymer. The flat surface and some cracks on

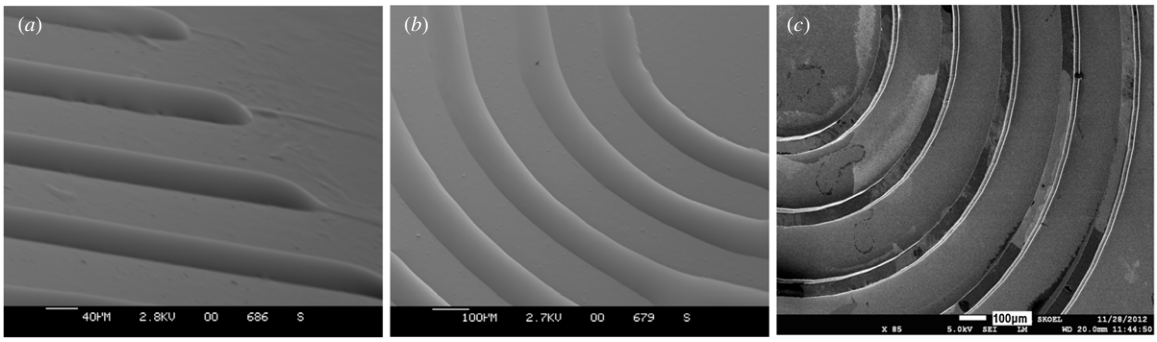

Figure 5. (*a*) SEM image of the fabricated straight polymeric waveguide core array with a width of 50 μm, a height of 10 μm and a pitch of 250 μm fabricated in the UV-cured polymer LightLink^{TM} XP-6701 (*A–Z*); (*b*) SEM image of the fabricated curved waveguide core array with the same width and height as those of (*a*); (*c*) SEM image of the nickel mold for the waveguide core array fabrication. The mold for the waveguide core has a binary shape with a width of 50 μm, a height of 50 μm and a pitch of 250 μm. The electric field strength used here is 10 V μm^{-1} and the gap between master and the surface of the polymer is 30 μm.

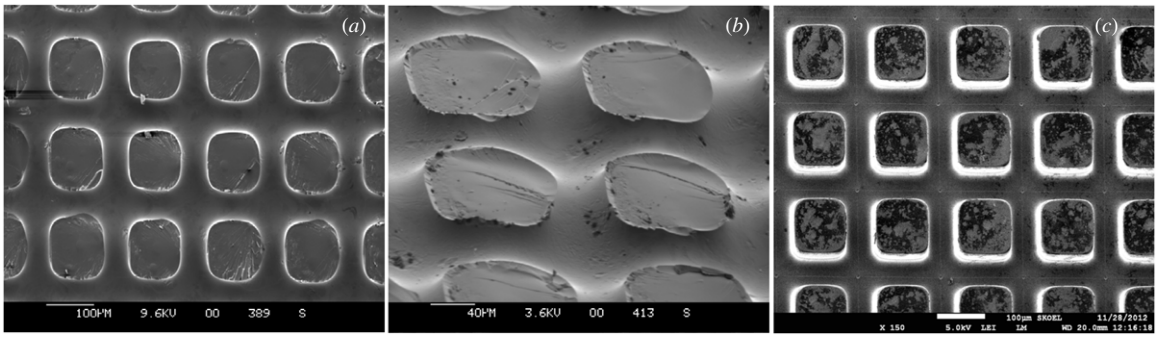

Figure 6. SEM images of square pillar array with a width of 100 μm and a pitch of 170 μm fabricated in the polymer (figure 6(*a*)–(*b*)) and SEM image for the nickel master (figure 6(*c*)). The electric field strength used here is 10 V μm^{-1} and the gap between the master and the polymer surface is 15 μm. The mold for the square pillar array has a binary shape and each pillar has a width of 100 μm and a height of 70 μm. The pillar pitch for the mould is 170 μm.

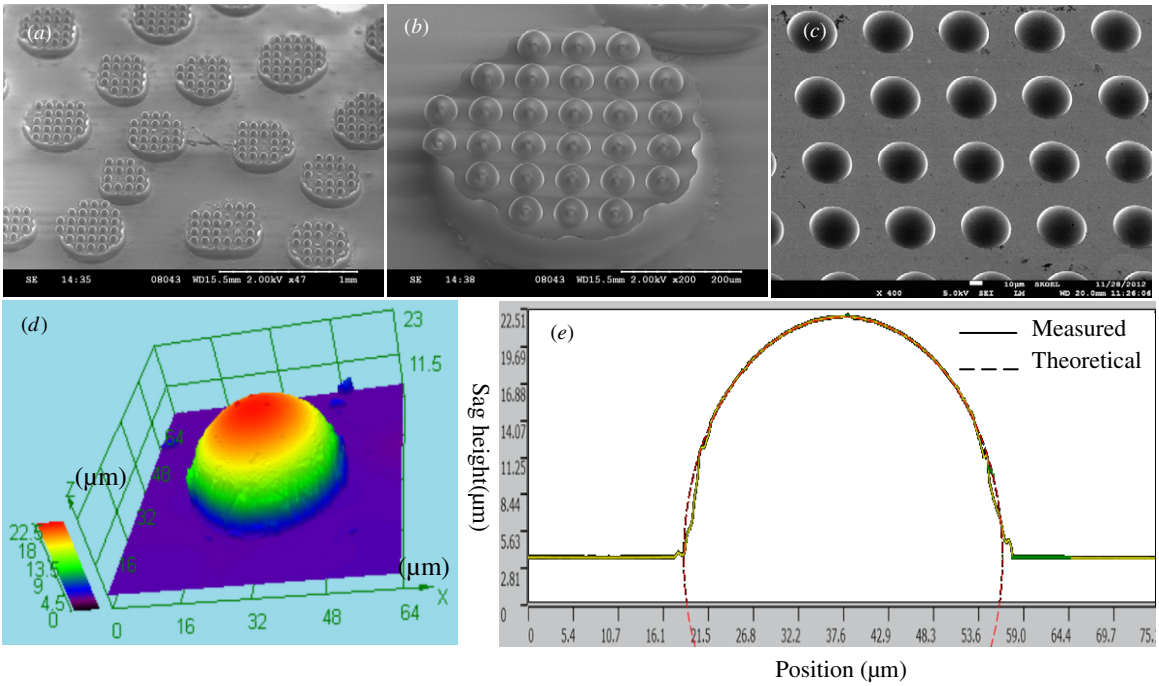

Figure 7. SEM images of the self-assembled islands with microlens array on the top fabricated in PDMS (figures 7(*a*)–(*b*)), SEM images of the corresponding nickel mold (figure 7(*c*)) and 3D and 2D surface profiles of the fabricated microlens measured by laser scanning confocal microscope (figures 7(*d*)–(*e*)). The electric field strength used here is 10 V μm^{-1} and the gap between the master and the polymer surface is 20 μm. The mould has a pattern of concave microlens arrays with a pitch of 60 μm and each lens has a diameter of 40 μm and a depth of 19 μm.

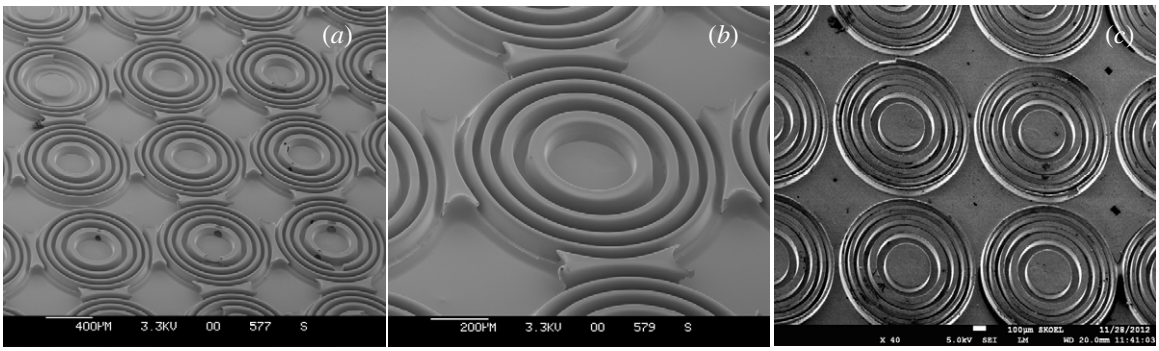

Figure 8. SEM images of binary zone-plate array fabricated in PDMS (figures 9(*a*)–(*b*)) and the corresponding nickel mold (figure 9(*c*)). The electric field strength used here is 10 V μm^{-1} and the gap between the master and the polymer surface is 20 μm. The mould has a pattern of concave microlens array with a pitch of 1115 μm and each lens has an outer diameter of 1065 μm and a height of 70 μm.

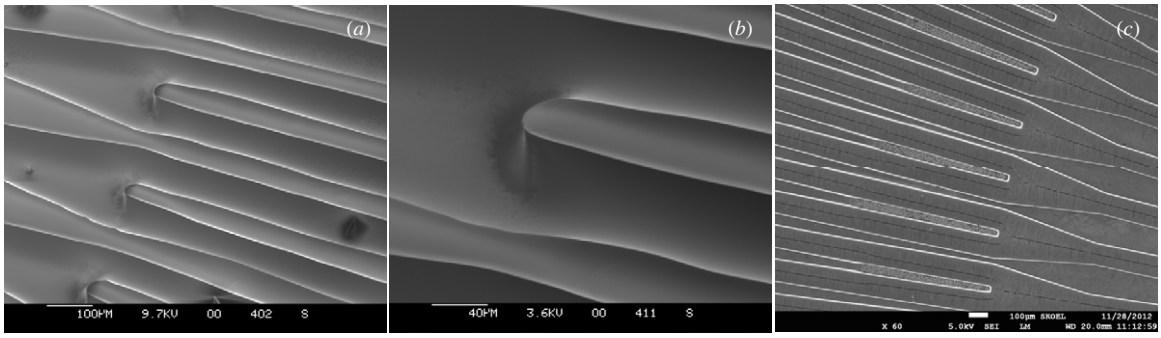

Figure 9. SEM images of the microchannels formed in the polymer by electric-field-induced lithography (figures 9(*a*)–(*b*)) and the corresponding nickel mold (figure 9(*c*)). The electric field strength used here is 10 V μm^{-1} and the gap between the master and the polymer surface is 20 μm. The mold has a pattern of microchannels with a width of 100 μm and a depth of 70 μm.

the top of the structures are due to the contact formed by the polymeric structure with the nickel master and the release of the structure after annealing, respectively. Figure 7 shows arrays of 40 μm diameter microlenses rested on the top of the self-assembled islands fabricated in polydimethylsiloxane (PDMS, sylgard 184, Dow Corning). This experiment was conducted with PDMS in a liquid state prepared by mixing ten volumes of curing agent with one volume of PDMS monomers. The process parameters were similar with those of experiments conducted with the novolac-based polymer. The self-assembled islands are formed as the air gap between the master electrode and the substrate is so large that the master electrode actually acts like a flat electrode. In this case, the self-assembled islands with the feature size much larger than that in the master electrode are formed in the polymer. Once the self-assembled polymeric islands touch the master electrode, the excessive polymer flows into and fills up the cavity array with a concave spherical surface to form the microlens array rested on the top of the islands. It is worth pointing out that the manufacturing process is not mature yet and defects as evidenced by the absence of some microlenses on some islands can be seen in figure 7(*a*). More work needs to be conducted to make this process more robust and reliable. The dark spots appearing on the microlenses in figure 7(*b*) are due to the accumulation of the electron charge on the surface of the lenses, which could be eliminated by over coating a thin layer of quality conductive film before observation under SEM. Figures 7(*d*)–(*e*) show the 3D and 2D surface profiles of a single microlens measured by a laser scanning confocal microscope (BX61, Olympus). As can be seen from figure 7(*e*), the measured surface profile matches with the theoretical spherical profile very well. The largest deviation of the measured curve to the theoretical one is only 1 μm. Figure 8 shows the binary Fresnel zone plate with a height of 90 μm fabricated in PDMS. As the smallest width of the ring is only 20 μm, an aspect ratio of 4.5:1 has been achieved. Dark features appearing in figure 8 mean the defects, which were probably caused by the breakage during the separation of the mold from the fabricated microstructures. This can be eliminated by modifying the surface of the mold to be hydrophobic to reduce the chance of the breakage happening during the separation.

In the above experiment, as the induced microstructure touches the electrode, the breakage of the microstructure occurs during its separation from the mould. This problem can be overcome by modifying the surface of the master electrode to be hydrophobic. A self-assembled monolayer is formed on the nickel master surface to change its wettability, which is achieved by the immersion of the nickel master into the solution of a 5 mM of octadecanethiol (ODT) in toluene. The breakage of the induced microstructure can be avoided as shown in figure 10 where the fabricated microstructure has a reasonably smooth surface on the sidewall as well as on the top surface.

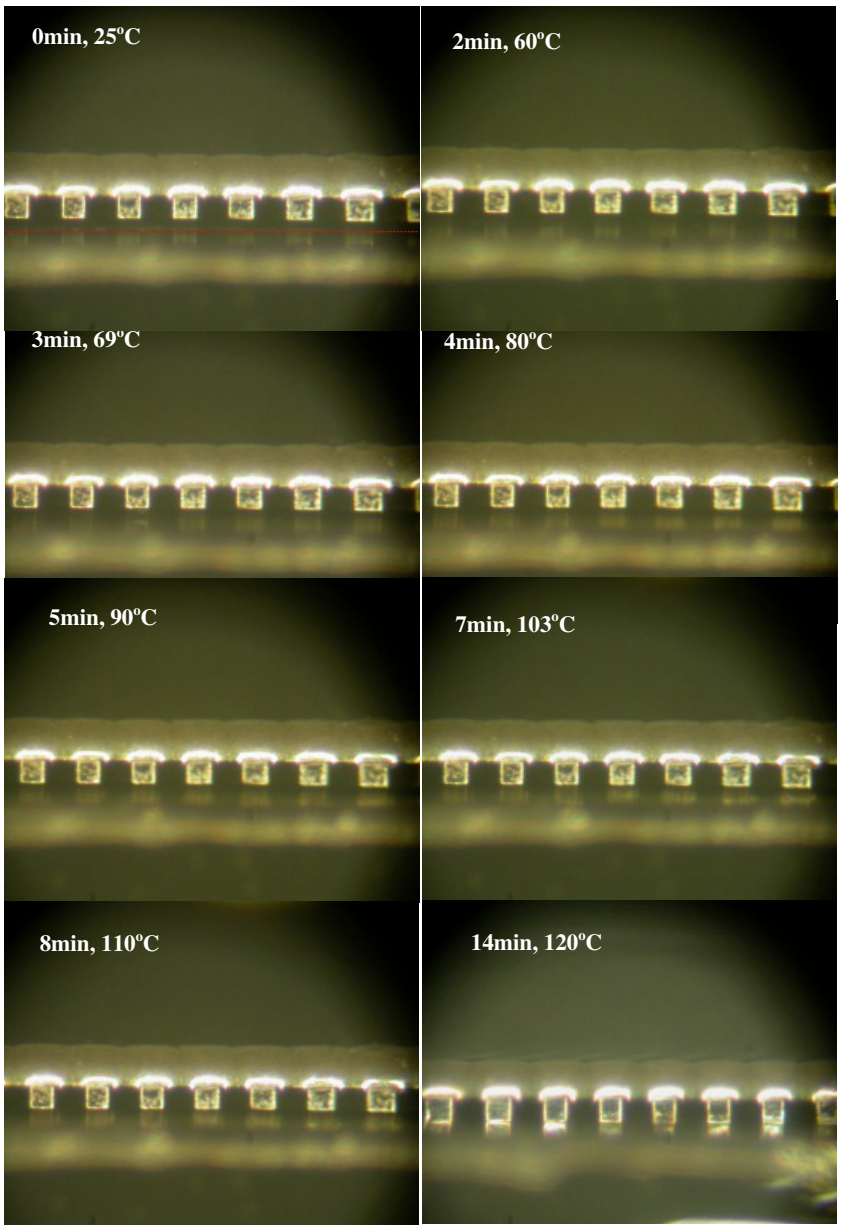

Figure 10. A series of images taken by a digital camera shows the polymer growth process. The broken line on the first figure indicates the interface between the polymer and air.

4. Monitoring the fabrication process

Monitoring the polymer growth in real time during electrostatic-induced lithography is a helpful tool to understand the process. Because the nickel master and the wafer are opaque to visible light, it is not possible to observe the polymer growth from the top or from underneath. One possible way is to observe the process from the side. The following approach was used to achieve this. An Olympus optical microscope with a large field of view equipped with a ring light head was used to observe the polymer growth in real time. The experimental setup to demonstrate this is similar to the setup depicted in figure 1 except that the air gap was 30 μm and an ac voltage of 250 V peak-to-peak was applied with a frequency of 50 Hz. Since the formation of the microstructures in the polymer is obtained by the electrostatic field distribution, the alternative voltage does not change the heterogeneity nature of the electric field generated by the patterned mould, therefore the polymer moves toward the strong electric field area irrespective of the frequency of the applied voltage. The observations were started from the time when the temperature of the hotplate reached 25 °C. A series of images shown in figure 10 were taken by a digital camera at different time intervals after the hotplate was switched on.

As can be seen from the picture taken at 25 °C, the interface of the polymer and air, shown by a line drawn on the first photograph, is somewhat clear. However, after 2 min at 60 °C, the interface becomes blurred. After 3 min at 69 °C, the polymer growth starts occurring. After 4 min at 80 °C, the

polymer growth can be seen very clearly. At 5 and 7 min, the polymer growth continues and the grown polymer has touched the top electrode in some areas due to the unevenness of the gap. After 8 min at 110 °C, the polymer had touched the top electrode in most of the area. Finally, after 14 min at 120 °C, the polymer had touched the whole of the top electrode. The polymer growth occurs very fast, normally a few minutes after the temperature reaches certain temperatures (here 69 °C). The whole growth process only takes about 15 min, suggesting that it is possible to reduce the whole process time from 1 h to 15 min or less.

5. Conclusions

In conclusion, the paper presents the process of generating microstructures using electrostatic-induced lithography. Microchannels and other microstructures with very smooth side walls have been fabricated in thick resist. The electrostatic-induced polymer growth has been monitored in real time and shows that the formation of the microstructure formation can be achieved within just 15 min for the case reported in this paper. This technology presented is proven to be a simple, flexible and a cost-effective solution for microfabrication, which can be of use in various applications which include microelectronics, photonics, MEMS, etc.

Acknowledgments

The authors acknowledge funding from the British Engineering and Physical Sciences Research Council (EPSRC) through the IeMRc flagship project entitled SMART MICROSYSTEMS. Financial contributions from Natural Science Foundation of China under grant numbers 90923036 and 60977041, Ministry of Sciences and Technology of China with grant number 2011DFA50590 as well as the 100 Talents Program of Chinese Academy of Sciences are also acknowledged.

References

[1] Kim H and Bankoff S G 1992 The effect of an electrostatic field on film flow down an inclined plane *Phys. Fluids* A **4** 2117–30

[2] Schaffer E, Thurn-Albrecht T, Russell T P and Steiner U 2000 Electrically induced structure formation and pattern transfer *Nature* **403** 874–7

[3] Lin Z, Kerle T, Baker S M and Hoagland D A 2001 Electric field induced instabilities at liquid/liquid interfaces *J. Chem. Phys.* **114** 2377–81

[4] Schaffer E, Thurn-Albrecht T, Russell T P and Steiner U 2001 Electrohydrodynamic instability in polymer films *Europhys. Lett.* **53** 518–24

[5] Salac D, Lu W, Wang C-W and Sastry A M 2004 Pattern formation in a polymer thin film induced by an in-plane electric field *Appl. Phy. Lett.* **85** 1161–3

[6] Shankar V and Sharma A 2004 Instability of the interface between thin fluid films subjected to electric fields *J. Colloid Interface Sci.* **274** 294–308

[7] Craster R V and Matar O K 2005 Electrically induced pattern formation in thin leaky dielectric films *Phys. Fluids* **17** 032104

[8] Kim D and Lu W 2006 Interface instability and nanostructure patterning *Comput. Mater. Sci.* **38** 418–25

[9] Uma B and Usha R 2008 A thin conducting viscous film on an inclined plane in the presence of a uniform normal electric field: bifurcation scenarios *Phys. Fluids* **20** 032102

[10] Tseluiko D, Blyth M G, Papageorgiou D T and Vanden-Broeck J-M 2008 Electrified viscous thin film flow over topography *Phys. Fluids* **20** 042103

[11] Tseluiko D, Blyth M G, Papageorgiou D T and Vanden-Broeck J-M 2008 Electrified viscous thin film flow over topography *J. Fluid Mech.* **597** 449–75

[12] Wu N and Russel W B 2009 Micro- and nano-patterns created via electrohydrodynamic instabilities *Nano Today* **4** 180–92

[13] Srivastava S, Sankar R P D, Wang C, Bandyopadhyay D and Sharma A 2010 Electric field induced microstructures in thin films on physicochemically heterogeneous and patterned substrates *J. Chem. Phys.* **132** 174703

[14] Pattader P S G, Banerjee I, Sharma A and Bandyopadhyay D 2011 Multiscale Pattern Generation in Viscoelastic Polymer Films by Spatiotemporal Modulation of Electric Field and Control of Rheology *Adv. Funct. Mater.* **21** 324–35

[15] Tian E M, Svobodny T P and Philips J D 2011 Thin liquid film morphology driven by electro-static field *Appl. Math. Mech.* **32** 1039–46

[16] El-Sayed M F, Moussa M H M, Hassan A A A and Hafez N M 2011 Electrohydrodynamic instability of two thin viscous leaky dielectric fluid films in a porous medium *Appl. Math.* **2011** 498718

[17] Pease Leonard F III and Russel W B 2002 Linear stability analysis of thin leaky dielectric films subjected to electric fields *J. Non-Newton. Fluid Mech.* **102** 233–50

[18] Lin Z, Kerle T and Russell T P 2002 Structure Formation at the interface of liquid/liquid bilayer in electric field *Macromolecules* **35** 3971–76

[19] Russell T P, Lin Z, Schäffer E and Steiner U 2003 Aspects of electrohydrodynamic instabilities at polymer interfaces *Fiber Polym.* **4** 1–7

[20] Pease L F III and Russel W B 2003 Electrostatically induced submicron patterning of thin perfect and leaky dielectric films: a generalized linear stability analysis *J. Chem. Phys.* **118** 3790–803

[21] Pease L F III and Russel W B 2004 Limitations on length scales for electrostatically induced submicrometer pillars and holes *Langmuir* **20** 795–804

[22] Verma R, Sharma A, Kargupta K and Bhaumik J 2005 Electric field induced instability and pattern formation in thin liquid films *Langmuir* **21** 3710–21

[23] Wu N, Peas L F III and Russel W B 2005 Electric-field-induced patterns in thin polymer films: weakly nonlinear and fully nonlinear evolution *Langmuir* **21** 12290–302

[24] Wu N and Russel W B 2006 Electrohydrodynamic instability of dielectric bilayers: kinetics and thermodynamics *Ind. Eng. Chem.* **45** 5455–65

[25] Tomar G, Shankar V, Sharma A and Biswas G 2007 Electrohydrodynamic instability of a confined viscoelastic liquid film *J. Non-Newton. Fluid Mech.* **143** 120–30

[26] Sarkar J, Sharma A and Shenoy V B 2008 Electric-field induced instabilities and morphological phase transitions in soft elastic films *Phys. Rev.* E **77** 031604

[27] Bandyopadhyay D, Sharma A, Thiele U and Sankar R P D 2009 Electric-field-induced interfacial instabilities and morphologies of thin viscous and elastic bilayers *Langmuir* **25** 9108–18

[28] Esmaeeli A and Reddy M N 2011 The electrohydrodynamics of superimposed fluids subjected to a nonuniform

transverse electric field International *J. Multiphase Flow* **37** 1331–47
[29] Yu W *et al* 2010 High-aspect-ratio metal microchannel plates for microelectronic cooling applications *J. Micromech. Microeng.* **20** 025004
[30] Hin T Y, Liu C, Conway P P, Yu W, Cargill S and Desmulliez M P Y 2010 Fabrication of a polymeric optical waveguide-on-flex using electrostatic-induced lithography *IEEE Photon. Technol. Lett.* **22** 957–9